

- (9) H. C. Snow, R. Serlin, and C. E. Strouse, *J. Am. Chem. Soc.*, **97**, 7230–7237 (1975).
- (10) Of the two H<sub>2</sub>O molecules reported by Strouse, only the one coordinated to magnesium was used in the studies reported here.
- (11) T. Koopmans, *Physica*, **1**, 104–113 (1933).
- (12) S. G. Boxer, G. L. Closs, and J. J. Katz, *J. Am. Chem. Soc.*, **96**, 7058–7066 (1974).
- (13) J. H. Fuhrhop, *Struct. Bonding (Berlin)*, **18**, 1–67 (1974).
- (14) Y. Nakato, T. Chiyoda, and H. Tsubomura, *Bull. Chem. Soc. Jpn.*, **47**, 3001–3005 (1974).
- (15) J. R. Harbour and G. Tollin, *Photochem. Photobiol.*, **19**, 69–74 (1974).
- (16) L. L. Shipman, T. M. Cotton, J. R. Norris, and J. J. Katz, *J. Am. Chem. Soc.*, in press.
- (17) This has been observed by G. M. Maggiora, *J. Am. Chem. Soc.*, **95**, 6555–6559 (1973).
- (18) J. R. Norris, R. A. Uphaus, H. L. Crespi, and J. J. Katz, *Proc. Natl. Acad. Sci. U.S.A.*, **68**, 625–628 (1971).
- (19) D. C. Borg, J. Fajer, R. H. Felton, and D. Dolphin, *Proc. Natl. Acad. Sci. U.S.A.*, **67**, 813–820 (1970).
- (20) D. Dolphin and R. H. Felton, *Acc. Chem. Res.*, **7**, 26–32 (1974).
- (21) For a description of some of the implications of the charge distribution for chlorophyll *a* dimerization, see L. L. Shipman, T. R. Janson, R. J. Ray, and J. J. Katz, *Proc. Natl. Acad. Sci. U.S.A.*, **72**, 2873–2876 (1975).
- (22) See L. L. Shipman and R. E. Christoffersen, *Chem. Phys. Lett.*, **15**, 469–474 (1972), for a detailed discussion of electron population analysis in symmetrically orthogonalized FSGO basis sets.
- (23) For an initial report of this effect, see D. Spangler, R. McKinney, R. E. Christoffersen, G. M. Maggiora, and L. L. Shipman, *Chem. Phys. Lett.*, **36**, 427–431 (1975).
- (24) R. C. Dougherty, H. H. Strain, and J. J. Katz, *J. Am. Chem. Soc.*, **87**, 104–109 (1965).
- (25) F. K. Fong, *J. Am. Chem. Soc.*, **97**, 6890–6892 (1975).

## Energy Dependence of the Radiationless Deactivation Rate for the Azulene System Probed by the Effect of External High Pressure

Dean J. Mitchell, Harry G. Drickamer,\* and Gary B. Schuster\*

*Contribution from the School of Chemical Sciences and the Materials Research Laboratory, University of Illinois, Urbana, Illinois 61801. Received April 7, 1977*

**Abstract:** The pressure dependence of the fluorescence of azulene and several of its derivatives was studied over a 130-kbar range. The efficiency of fluorescence from both the second and first excited singlet states was pressure dependent as was the relative energy of these states. It was shown that the fluorescence efficiency is limited by internal conversion from both excited singlet states. Furthermore, the rate of internal conversion was observed to depend strongly on the energy separating the relevant states.

Interest in the behavior of electronically excited azulene systems has been focused mainly on the rates of nonradiative decay from the excited singlet states of these molecules. Two unusual aspects of the radiationless decay from this chromophore have been noted. First, the second excited singlet state ( $S_2$ ) of azulene fluoresces with a quantum efficiency of 0.02.<sup>1</sup> This unusually efficient anomalous fluorescence has been attributed to, among other things, inefficient competitive internal conversion to the first excited singlet state ( $S_1$ ). Second,  $S_1$  of azulene is essentially completely nonemissive. Fluorescence from this state has only recently been detected through the application of high-powered laser excitation.<sup>2</sup> Furthermore, the lifetime of  $S_1$  has been measured by several different picosecond techniques. Although the exact magnitude of the  $S_1$  lifetime varies depending upon the measuring procedure, it is clear that it is less than ca. 5 ps.<sup>3</sup> The rapid nonradiative relaxation of  $S_1$  has been attributed to either internal conversion, intersystem crossing, or some combination of these two deactivation pathways.<sup>4</sup>

The application of external high pressure to the investigation of electronically excited molecules can reveal much about the pathways interconnecting the various states.<sup>5</sup> We have shown that the effect of application of external pressure to organic systems can be interpreted in terms of the interactions between the states of the molecule and the environment. Pressure can be used to probe the active decay modes of an electronically excited substance. We have shown that pressure-dependent behavior can be analyzed by a configuration coordinate model in which changes in vibrational force constants, relative potential energy, and position on the relevant intermolecular configuration parameter explain pressure-dependent behavior.<sup>6</sup> Moreover, in suitable systems it has proven possible to isolate

these three parameters and analyze the pressure-dependent behavior of each.

In this paper we report our study of the pressure dependence of the emission and absorption for azulene and several of its derivatives. Primarily, the relationship between the relative energetic separation of the singlet states of these compounds and the efficiency of various energy degradation routes is probed. In addition, phosphorescence from suitably substituted azulenes permits further evaluation of the triplet state and the importance of competitive internal conversion and intersystem crossing from  $S_1$ .

### Experimental Section

Azulene (**1**) (Aldrich) was purified by column chromatography (alumina) followed by recrystallization from methanol. Substituted azulenes **2**, **3**, **4**, and **6** were prepared by the procedure of Nozoe.<sup>7</sup> Bromo-substituted azulenes **5** and **7** were prepared using the procedure described by Eber.<sup>8</sup> All substituted azulenes were purified by chromatography and recrystallization before use.

Purification and polymerization of poly(methyl methacrylate) (PMMA) and polystyrene (PS) were described previously.<sup>5</sup> The compounds and plastic were dissolved in methylene chloride, forming approximately 0.05 M, 0.2 mm thick films after solvent evaporation. Emission was also investigated in solution of approximately  $10^{-4}$  M.

The high-pressure cells and emission equipment, as well as methods of processing and analyzing the data, are described elsewhere.<sup>9</sup> The low-temperature techniques were developed by Tyler.<sup>10</sup> The transmission efficiency of the high-pressure cell for measurements below 40 kbar is independent of pressure. For the higher pressure range the transmission efficiency was calibrated using 9,10-diphenylanthracene (DPA) in PMMA, which has a fluorescence quantum yield near unity.<sup>11</sup> Above 100 kbar, however, the quantum yield of DPA appears

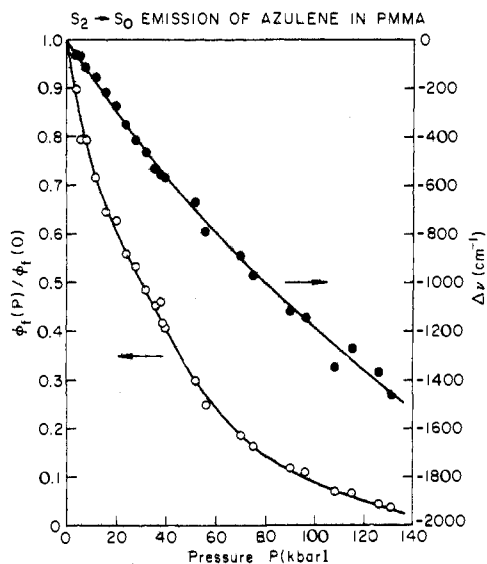


**Figure 1.** Pressure dependence of the energy of the emission peak maximum (solid circles) and the relative fluorescence quantum yield (open circles) for the  $S_2 \rightarrow S_0$  transition of azulene in PMMA.

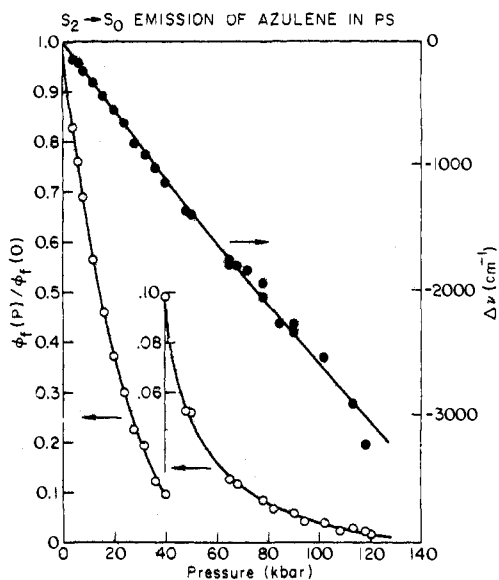


**Figure 2.** Pressure dependence of the energy of the emission peak maximum (solid circles) and relative fluorescence quantum yield (open circles) for the  $S_2 \rightarrow S_0$  transition of azulene in PS.

to fall, and the calibration was extrapolated based on an independent calibration.<sup>10</sup>

The quantum yields at atmospheric pressure were determined relative to DPA by taking the integrated intensity of the front surface emission from plastic films. The excitation wavelength was set at 334 nm. The concentrations and path lengths were sufficient to ensure that essentially all the incident radiation was absorbed. It was shown that the emission efficiency was not dependent upon the energy difference between the excitation and absorption peak energy for optical densities meeting this criterion.

## Results

The emissive properties of azulenes **1**–**7** were studied as a function of pressure under a variety of conditions. The effect of the pressure variation on the luminescent intensity and on energies of the luminescing states was monitored. Fluorescent emission from the compounds studied ranges from dominant  $S_2 \rightarrow S_0$  for azulene (**1**) to predominant  $S_1 \rightarrow S_0$  fluorescence for dicarboethoxyaminoazulene **6**. The quantum efficiencies for the azulenes studied in this work were determined at room

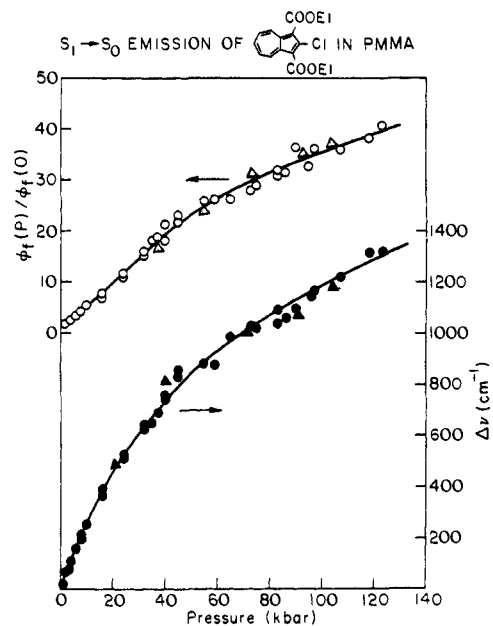
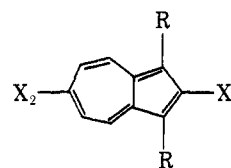


**Figure 3.** Pressure dependence of the fluorescence peak shift and quantum yield for the  $S_1 \rightarrow S_0$  transition of dicarboethoxychloroazulene **4** in PMMA. The circles correspond to excitation into  $S_2$  and the triangles apply to excitation into  $S_1$ .

**Table I.** Quantum Yields<sup>a</sup> and Emission Maxima of Azulene Derivatives at 1 atm in Plastic Media

Compd	Medium	Transition	$\nu_{\max}$ , $\text{cm}^{-1}$	$\phi_f^a$
1	PMMA	$S_2 \rightarrow S_0$	26 670	0.027
1	PS	$S_2 \rightarrow S_0$	26 520	0.028
2	PMMA	$S_2 \rightarrow S_0$	26 330	0.0097
3	PMMA	$S_2 \rightarrow S_0$	25 510	0.0061
4	PMMA	$S_2 \rightarrow S_0$	24 810	0.000079
4	PS	$S_2 \rightarrow S_0$	24 790	0.000048
5	PMMA	$S_2 \rightarrow S_0$	24 640	0.000052
4	PMMA	$S_1 \rightarrow S_0$	15 230	0.00045
4	PS	$S_1 \rightarrow S_0$	15 210	0.00055
5	PMMA	$S_1 \rightarrow S_0$	15 160	0.00044
6	PMMA	$S_1 \rightarrow S_0$	16 440	0.0036
6	PS	$S_1 \rightarrow S_0$	15 946	0.0065
7	PMMA	$S_1 \rightarrow S_0$		0.0008

<sup>a</sup> All yields are determined relative to that of 9,10-diphenylanthracene in PMMA, which is taken to be 0.99.<sup>11</sup>



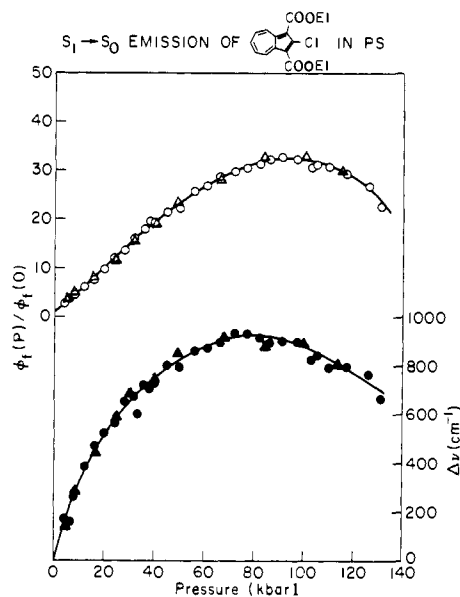
- 1 R = X<sub>1</sub> = X<sub>2</sub> = H
- 2 R = X<sub>1</sub> = H, X<sub>1</sub> = Cl
- 3 R = X<sub>2</sub> = H, X<sub>1</sub> = I
- 4 R = CO<sub>2</sub>Et, X<sub>1</sub> = Cl, X<sub>2</sub> = H
- 5 R = CO<sub>2</sub>Et, X<sub>1</sub> = Cl, X<sub>2</sub> = Br
- 6 R = CO<sub>2</sub>Et, X<sub>1</sub> = NH<sub>2</sub>, X<sub>2</sub> = H
- 7 R = CO<sub>2</sub>Et, X<sub>1</sub> = NH<sub>2</sub>, X<sub>2</sub> = Br

temperature and atmospheric pressure by comparison with DPA. These data along with the corrected emission maxima are collected in Table I.

The effect of external pressure on PMMA and PS solutions of the azulenes is shown in Table II. In general, as the external pressure increases, the position of the  $S_2 \rightarrow S_0$  emission maximum shifts to lower energy indicating a decrease in the energy separating these two states. In every case studied the dimini-

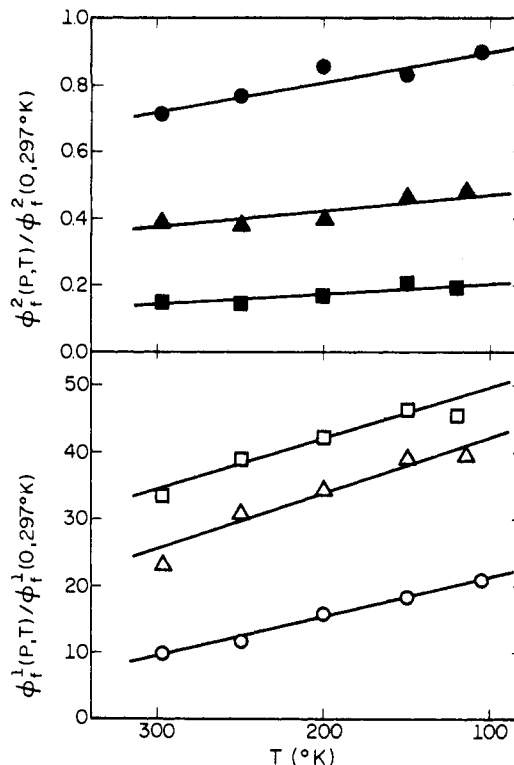
**Table II.** Effect of Pressure on Emission Energy and Fluorescence Yield

Compd	Medium	Transition	$\phi_f(P)/\phi_f(O)$								$\Delta\nu, \text{cm}^{-1}$					
			Pressure, kbar								Pressure, kbar					
			10	20	40	60	80	100	120	10	20	40	60	80	100	120
1	PMMA	$S_2 \rightarrow S_0$	0.750	0.605	0.400	0.245	0.145	0.090	0.050	-155	-300	-560	-795	-1005	-1190	-1365
1	PS	$S_2 \rightarrow S_0$	0.625	0.375	0.0950	0.0315	0.0155	0.0075	0.0030	-290	-560	-1100	-1610	-2100	-2570	-3040
2	PMMA	$S_2 \rightarrow S_0$	0.730	0.590	0.420	0.300	0.210	0.140	0.075	-180	-335	-570	-755	-910	-1040	-1170
4	PMMA	$S_2 \rightarrow S_0$	0.820	0.710	0.440	0.305	0.185	0.120		-110	-215	-395	-540	-665	-770	
4	PS	$S_2 \rightarrow S_0$	0.875	0.750	0.500					-140	-275	-550				
5	PMMA	$S_2 \rightarrow S_0$	0.860	0.735	0.555	0.430	0.340	0.270	0.215	-250	-420	-640	-760	-830	-880	-910
4	PMMA	$S_1 \rightarrow S_0$	5.3	9.8	19.0	26.0	31.5	35.5	39.0	225	450	735	925	1070	1185	1290
4	PS	$S_1 \rightarrow S_0$	5.5	10.0	19.5	27.0	31.5	32.0	28.5	320	515	750	880	922	878	770
5	PMMA	$S_1 \rightarrow S_0$	2.45	3.75	5.60	6.70	7.40	7.90	8.20	130	250	420	550	680	790	885
6	PMMA	$S_1 \rightarrow S_0$	1.95	2.85	4.60	6.15	7.20	8.00	8.40	175	330	590	785	945	1090	1220
6	PS	$S_1 \rightarrow S_0$	1.60	2.20	2.90	3.10	3.05	2.80	2.30	90	155	285	380	430	430	370

**Figure 4.** Pressure dependence of the fluorescence peak shift and quantum yield for the  $S_1 \rightarrow S_0$  transition of dicarboethoxychloroazulene **4** in PS. The circles correspond to excitation into  $S_2$  and the triangles apply to excitation into  $S_1$ .

tion of the  $S_2 \rightarrow S_0$  energy gap is associated with a reversible decrease in the fluorescence intensity from the upper excited state. For azulene (**1**) the pressure dependence of the anomalous fluorescence in PMMA is shown in Figure 1 and in PS in Figure 2. Significantly, the shift in the observed energy of emission is more than twice as large in PS as in PMMA for a given pressure increase.

The pressure dependence of the emission from  $S_2$  for dicarboethoxychloroazulene **4** is qualitatively similar to that of azulene itself (Table II). However, this compound also emits from  $S_1$  with detectable intensity. The pressure dependence of the  $S_1$  emission from **4** is shown for PMMA solution in Figure 3 and for PS solution in Figure 4. As is the case for azulene  $S_2$  emission, the  $S_1$  emission of **4** is strongly pressure dependent. In PMMA, as the external pressure increases, the position of the emission maximum moves blue indicating that, in this case, increased pressure increases the energy gap between  $S_1$  and  $S_0$ . It is important to note that the luminescent efficiency from the first excited singlet of **4** increases with increasing pressure. The pressure response of  $S_1$  for substituted azulene **4** in PS is particularly revealing. In the lower pressure range the emission shifts blue, just as in PMMA, but at pressures above ca. 80 kbar the direction of the shift for the emission maximum reverses and shifts red. The efficiency of fluorescence from  $S_1$  of **4** in PS follows the emission shift closely,

**Figure 5.** Effect of temperature on the fluorescence quantum yields for dicarboethoxychloroazulene **4** in PMMA. The solid symbols correspond to the transition  $S_2 \rightarrow S_0$ , and the open symbols to the  $S_1 \rightarrow S_0$  transition. The circles, triangles, and squares correspond to pressures of 20, 50, and 90 kbar, respectively.

increasing as the emission shifts blue and decreasing when the emission shifts red. Furthermore, it was shown that the pressure dependence of the  $S_1$  emission of **4** was unchanged if the excitation was switched from initially populating  $S_1$  to direct excitation via absorption into  $S_2$ .

The pressure-dependent behavior of the fluorescence for chlorobromoazulene **5** and aminoazulene **6** is qualitatively similar to **4**. The  $S_1$  states of both **5** and **6** shift toward higher energy in PMMA solution as the pressure increases. Moreover, the increase in fluorescence efficiency observed in **4** is paralleled in **5** and **6** (Table II).

The temperature dependence of the emission of dicarboethoxychloroazulene **4** was investigated at various pressures. Figure 5 shows the effect of temperature variation for both the  $S_1$  and  $S_2$  fluorescence of this compound in PMMA. At a given pressure the emission efficiency from both singlet states was found to increase in a uniform way as the temperature decreased from 300 to 100 K.

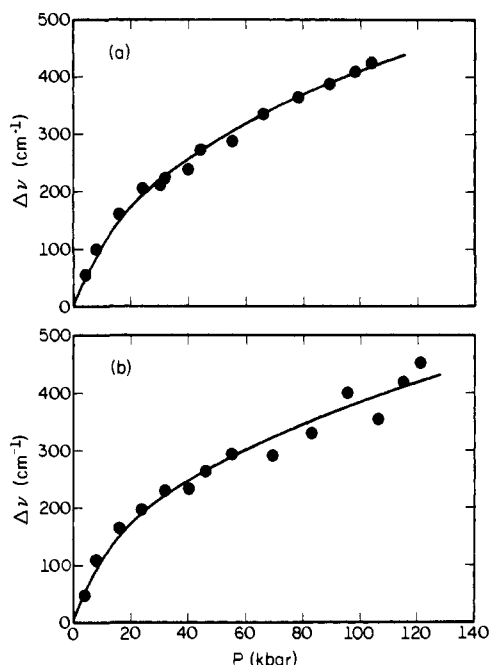


Figure 6. Pressure dependence of phosphorescence peak energy for di-carboethoxybromoaminoazulene 7 in (a) PMMA and (b) PS.

Table III. Pressure Dependence of Transitions for Chlorodicarboethoxyazulene 4

Medium	Transition	$(d\nu/dP)_0, \text{cm}^{-1}/\text{kbar}^a$
PMMA	$S_1 \rightarrow S_0$	+27
PMMA	$S_0 \rightarrow S_1$	0
PS	$S_1 \rightarrow S_0$	+35
PS	$S_0 \rightarrow S_1$	-10
PMMA	$S_2 \rightarrow S_0$	-11
PMMA	$S_0 \rightarrow S_2$	-12
PS	$S_2 \rightarrow S_0$	-14
PS	$S_0 \rightarrow S_2$	Negative

<sup>a</sup> The pressure derivative of the peak shift evaluated at zero pressure.

Investigation of the pressure dependence of the absorption spectrum of 4 revealed that the initial rate of shift for the absorption and emission to the  $S_1$  state differed significantly. The first derivative of the shift for 4 under various conditions is shown in Table III.

Bromo-substituted azulene 7 was observed to phosphoresce in PMMA and PS solution with a detectable intensity. The pressure dependence of the phosphorescence spectrum of this compound is shown in Figure 6. The phosphorescence intensity increases rapidly for the first 20 kbar. This effect has been attributed to the inhibition of diffusion and thereby oxygen quenching.<sup>12</sup> It was observed that at high pressure the phosphorescence quantum efficiency ( $\phi_p$ ) is less sensitive to pressure than the corresponding fluorescence. Moreover, the phosphorescence intensity under high-pressure conditions is approximately 50 times as great as the fluorescence for this compound in both PMMA and PS.

### Discussion

The effect of pressure on the excited state properties of azulene and its derivatives is easily understood in terms of a schematic configuration coordinate diagram which shows in a qualitative way the relationship between a displacement of the potential wells and the relative probability of radiationless relaxation (Figure 7). For a given displacement along the relevant configuration coordinate ( $\Delta_0$ ), as the energy of the

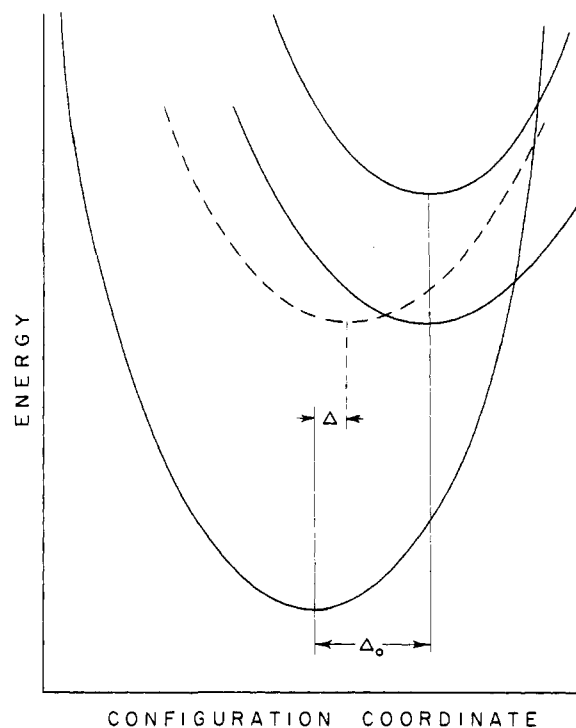


Figure 7. Generalized configuration coordinate diagram showing the effects of displacement of potential wells. Upper curves refer to configurationally displaced excited states of different energies and of displacements  $\Delta_0$  and  $\Delta$  (dashed).

excited state increases relative to the ground state, the height of the barrier to be crossed and the thickness for tunneling increase. In this diagram a blue shift of an emission peak with pressure would lead to an increase in emission intensity, and a red shift to a decrease in intensity. Similarly, a decrease in relative displacement along the configuration coordinate ( $\Delta_0 \rightarrow \Delta$ ) would decrease the probability of radiationless relaxation and increase emission intensity.

Pressure couples to the volume so that the configuration coordinate most affected in these experiments is the breathing mode of the system; it is an intermolecular coordinate, i.e., it involves the interaction of the azulene with the polymeric environment. This point is discussed in detail elsewhere.<sup>6,9</sup>

Both the vertical and horizontal displacements of the potential wells can in principle be calculated from the peak shift and the change in shape with pressure. The equations which relate the shift of the optical absorption and emission peaks to the configuration coordinate parameters are given by

$$(\delta h\nu)_a = PR\Delta + P^2 \frac{(R-1)}{2w^2} + \frac{R\Delta^2}{2}(w^2 - w_0^2) \quad (1)$$

$$(\delta h\nu)_e = \frac{P\Delta}{R} + \frac{P^2(R-1)}{2w^2R^2} - \frac{\Delta^2}{2}(w^2 - w_0^2) \quad (2)$$

where  $\delta$  refers to the change in a quantity between pressure  $P$  and 1 atm (effectively zero pressure),  $\Delta_0$  is the displacement at zero pressure, and  $R = (w'/w)^2$  is the ratio of the force constants of excited to ground state potential wells. Evaluation of these quantities requires relatively isolated absorption and/or emission peaks of simple symmetry.

A quantitative calculation of the emission efficiency requires that one consider the barrier height in the presence of configuration interaction, the tunneling probability, and possibly anharmonicity. Appropriate relationships have been developed by Struck and Fonger<sup>13</sup> and applied in quantitative way to high-pressure data for simple inorganic systems by Tyner.<sup>10</sup> Unfortunately, the absorption and emission spectra of azulene and its derivatives in PS and PMMA are far too complex to

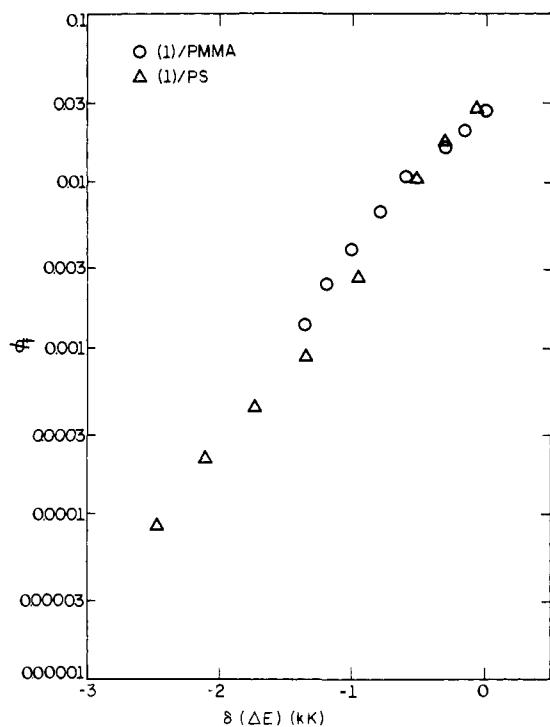


**Figure 8.** Correlation between the  $S_2$  fluorescence quantum yield and the change in the  $S_1 \rightarrow S_2$  energy gap for azulene in PMMA and PS.

analyze by this procedure. While such calculations are not possible for our data, the basic picture and ideas involved are useful for discussing our results.

In Figure 8, the dependence of  $\phi_f$  on the  $S_1$ - $S_2$  energy gap for emission from  $S_2$  to the ground state of azulene is shown. Since the 0-0 transitions are not resolved in the plastic media, we have chosen to represent the change in the energy gap,  $\delta(\Delta E)$ , by the shift of emission from  $S_2$  minus the shift of absorption to  $S_1$ . The radiative transition probability is not expected to be sensitive to pressure,<sup>14</sup> and if we neglect intersystem crossing (we will discuss this point more thoroughly), the rate of internal conversion changes approximately as the inverse of  $\phi_f$ . Figure 8 shows that the radiationless transition rate is nearly an exponential function of the energy gap. This dependence has previously been recognized.<sup>15-17</sup> Furthermore, the correspondence between the energy gap and the emission efficiency for azulene in PMMA and PS is the same. A similar result for the  $S_1$  emission of substituted azulenes **4** and **6** is shown in Figure 9. In this case the energy of the emission peak maximum,  $\nu_{\max}$ , is an indication of the energy gap between  $S_0$  and  $S_1$ . For comparison, a line is included in Figure 9 with a slope that approximates the dependence of the azulene  $S_2$  quantum yield on  $\delta(\Delta E)$ . It is clear that in spite of the obvious dissimilarities in the pressure dependence of emission from  $S_1$  and  $S_2$  of these compounds (indicating opposite displacements along the configuration coordinate), the correlation between  $\phi_f$  and  $\Delta E$  is not vastly different. In fact, the characteristics of  $S_1$  emission for compound **4** in PS, which goes through a maximum in the peak shift, are consistent when plotted in such a manner.

The pressure dependence of  $\phi_f$  is due to a change in the nonradiative rate of deactivation for both  $S_1$  and  $S_2$ . Our results indicate that  $\phi_f$  is very strongly correlated with the energy gap separating the relevant excited states as is clear from analysis of Figure 7. Moreover, the change in  $\phi_f$  with the energy gap appears to be independent of the medium, the particular substituents on the azulene ring, and most significantly on the singlet state from which the emission originates. These observations are consistent only with internal conversion as the

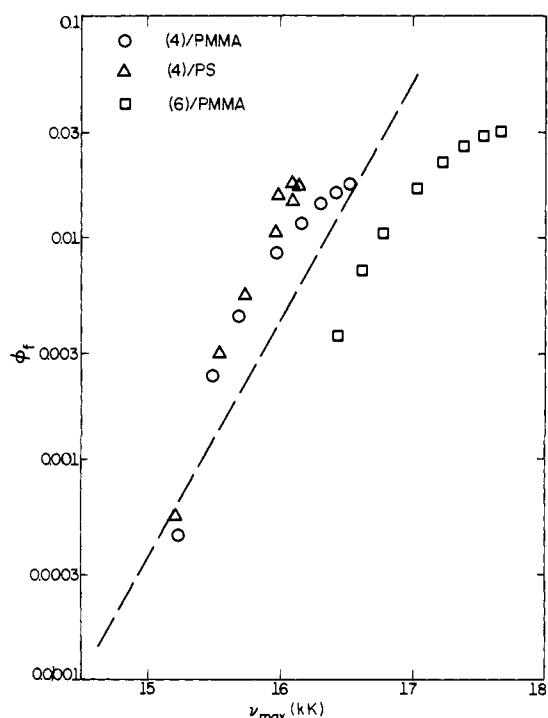


**Figure 9.** Dependence of the  $S_1$  fluorescence quantum yield on the peak maximum for azulenes **4** and **6**. The dashed line approximates the dependence of  $\phi_f$  upon the energy difference between  $S_1$  and  $S_2$  for  $S_2$  emission of azulene in polymeric environments.

major pathway competing with fluorescence from both  $S_2$  and  $S_1$  for these azulene derivatives.

The effect of heavy atom substitution on the emission spectra of the azulene molecule is shown in Table II. In spite of the fact that the  $S_1$ - $S_2$  energy gap of iodoazulene **3** is  $400\text{ cm}^{-1}$  smaller than that of chloroazulene **2**,<sup>17</sup> there is only a slight decrease in  $\phi_f$  for the iodine substituted compound. Similarly, we calculate the energy gap for the bromine substituted compound **5** to be  $100\text{ cm}^{-1}$  smaller than that of compound **4**, and again observe only a very small decrease in  $\phi_f$ . Thus, we are in agreement with previous conclusion that intersystem crossing is negligible relative to internal conversion as a mode of decay from  $S_2$  of azulene and these derivatives.<sup>17</sup>

It has been suggested that for azulene a significant fraction of molecules excited into  $S_1$  decay through the triplet manifold via intersystem crossing.<sup>1,4</sup> Our results appear to be at odds with this conclusion. Owing to the low yield and insensitivity of the photomultiplier tube at the appropriate energy, we were not able to detect emission from  $S_1$  of azulene. However, because the  $S_0$ - $S_1$  energy gap for compounds **4-7** are larger than that for azulene (implying smaller probabilities of internal conversion) and because the presence of nonbonding orbitals can only increase the rate of intersystem crossing, the yield of intersystem crossing for these compounds should represent an upper limit for that of azulene.

As noted in the discussion of the decay from  $S_2$ , one can infer from the correlation of  $\phi_f$  with the energy of emission from  $S_1$  that internal conversion is primarily responsible for the radiationless decay of  $S_1$ . In addition, we can estimate the ratio of the rates of intersystem crossing to internal conversion for dicarboethoxyaminoazulene **6** by making use of the heavy atom effect observed for the brominated compound **7**. It was found that the phosphorescence quantum yield for compound **7** is about 60 times greater than that for compound **6**. In general, the effect of heavy atom substitution is greater for  $S_1 \rightarrow T_1$  than for transitions from  $T_1$  to the ground state. Moreover, both radiative and nonradiative transitions from  $T_1$  to  $S_0$  are affected approximately equally. This implies that the rate of

intersystem crossing from  $S_1$  of **7** is approximately 60 times as great as that for compound **6**. We have also observed that  $\phi_f$  for azulene **6** is about four times as great as it is for azulene **7** in both methanol and PMMA. It is reasonable that the radiative transition rates for  $S_1 \rightarrow S_0$  of these very similar compounds are about equal. Since the emission maximum of **7** is  $200 \text{ cm}^{-1}$  lower in energy than for **6** we can make the conservative assumption that the rate of internal conversion for compound **6** is not greater than that for **7**. Now, applying this information to the calculated quantum yields of fluorescence for the two compounds, we conclude that for **6** the rate of internal conversion is no less than 20 times faster than the rate of intersystem crossing, i.e., the intersystem crossing yield is less than 5%. Since azulene **6** has the largest  $S_0 \rightarrow S_1$  energy gap of the compounds studied, this represents an upper limit to the yield of intersystem crossing. Indeed, heavy atom substitution does not appear to have any direct effect upon  $\phi_f$  for compound **4**.

One point which may be readily deduced from eq 1 and 2 is that the pressure derivative of the shift in energy for both absorption and emission between the same states must be of the same sign (but the magnitude of the slopes may differ). Since the initial shift of the absorption peak is approximately equal to the emission shift for  $S_2$  of **4** (see Table III), it can be concluded that both absorption and emission occur between the same ground and excited states (as is normally the case). Absorption to  $S_1$  of **4**, however, is independent of pressure in PMMA and shifts red in PS, while emission from  $S_1$  of this compound initially shifts blue in either medium. The pressure effect on the  $S_1$  emission is the same whether the molecule is initially excited into either  $S_1$  or  $S_2$ . This observation indicates that a relaxation process occurs within the lowest excited singlet state of compound **4** in either medium.

We cannot positively identify the nature of the relaxation mechanism in  $S_1$  of **4**. However, several characteristics of the  $S_1$  emission bear discussion. First, we have found that the ratio of the fluorescence quantum yield of  $S_1$  to  $S_2$  for **4** in the polymeric medium is about 8, whereas this ratio is less than 0.2 in ethanol at room temperature.<sup>8</sup> As shown in Figure 6, there is only a small temperature dependence for emission from either  $S_1$  or  $S_2$  in PMMA. The  $S_2$  emission intensity in ethanol is also relatively insensitive to temperature. The  $S_1$  emission intensity temperature dependence may be characterized by two coefficients. Above 77 K, the intensity increases rapidly with decreasing temperature; however, below this point the temperature coefficient is small (as in PMMA), yet the quantum yield remains far less than unity. Although it may be coincidental, in ethanol at 77 K and atmospheric pressure the ratio of  $\phi_f$  for  $S_1$  to  $\phi_f$  for  $S_2$  is about the same as that in the polymeric medium at 1 atm. These observations indicate that above 77 K, the  $S_1$  state of **4** in ethanol may decay by an activated crossing between states in addition to a tunneling mechanism, whereas in the plastic at or below room temperature, only the latter mechanism may be significant.

The intensity ratio for emission of  $S_1$  relative to  $S_2$  for **4** in toluene is similar to that in ethanol, in spite of the chemical similarities of toluene to PS. In toluene, the  $S_1$  emission intensity was observed to increase by a factor of 2 in 10 kbar. The ratio of intensities of  $S_1$  to  $S_2$  for **4** in glycerol is also like that in ethanol. There is only a modest increase of  $S_1$  emission intensity with pressure, although at the highest pressure (10 kbar) the solvent viscosity is about 2000 P.<sup>18</sup>

The activated relaxation process in  $S_1$  of **4** may be related to the permanent dipole moment that exists in the ground state of azulene in the direction of the five-membered ring. The direction of the dipole moment is observed to reverse in  $S_1$ .<sup>12</sup> Therefore, resonance with electron-withdrawing groups may destabilize  $S_1$  and rotation of the substituent out of conjugation may lower the energy of  $S_1$ . A second type of relaxation which

may occur is a reorientation of the solvent field. The importance of either of these processes is determined by the rate at which the system goes to the relaxed state relative to the rate of decay to the ground state. Any energy-lowering process in  $S_1$  will result in a decrease in the already small energy gap separating  $S_1$  and the ground state and hence an increase in the radiationless deactivation rate. One explanation for the difference between the  $S_1$  emission intensity of **4** in liquids and plastics is the occurrence of a relaxation in the former medium which is inhibited in the latter. As indicated above, we were not able to demonstrate the onset of such an effect for solvent viscosities less than 2000 P.

The effect of the environment upon the pressure dependence of the shift of the  $S_1$  absorption peak of **4** is similar to that of azulene. Absorption to the  $S_1$  state of azulene, which corresponds to a  $^1A \rightarrow ^1L_b$  transition, has been reported to shift blue with increasing pressure in ethanol.<sup>20</sup> In PMMA, we find that the shifts of this transition with pressure for both azulene and compound **4** to be negligible within the limits of our resolution ( $100 \text{ cm}^{-1}$ ) over a pressure range of 100 kbar. However, in PS the initial rates of shift are  $-5$  and  $-10 \text{ cm}^{-1}/\text{kbar}$ , respectively. The difference in the effect of these environments can be understood by considering the dipole moment of azulene which changes orientation upon excitation. The polar solvent field does not have time to reorient itself during the transition, so that repulsive interactions in the polar environment cancel the tendency to red shift as a result of dispersive interactions. Therefore, only nonpolar PS, where the polarizability is dominant, produces a significant red shift.

Finally, in Figure 6 the pressure dependence of the shift of the phosphorescence peak of **4** is seen to be approximately the same in PS and PMMA. A similar observation has been recorded for triphenylene phosphorescence.<sup>21</sup> This is in contrast to transitions between singlet states, which are generally more strongly red shifted in PS.

## Conclusions

The efficiency of fluorescence of the azulene systems studied appears to be determined in large part by the rate of competitive internal conversion from both  $S_2$  and  $S_1$ . In turn, the parameter of overriding importance influencing the rate of internal conversion is the energy separating the two states involved. Through the application of external high pressure, we have been able to vary the energy gap between the relevant states in a controlled and systematic way. The rate of internal conversion is observed to be a well-behaved function of this parameter. The radiationless deactivation efficiency correlates with the particular substituents on the azulene ring, and the direction in which the relative energy is moving. These results are most consistent with Franck-Condon factors controlling the rate of radiationless relaxation from both  $S_1$  and  $S_2$  for these azulenes.

In the case of dicarboethoxychloroazulene **4**, the observed difference in the direction of the initial pressure dependent energy shifts for absorption and emission of the  $S_0 \rightarrow S_1$  transition indicates that a reversible molecular reorganization occurs in the excited state. Since the absorption and emission shifts of  $S_2$  are similar, we conclude that the reorganization is occurring in  $S_1$ . Moreover, excitation into either  $S_2$  or  $S_1$  leads to the same result. A reasonable mechanism for the conformational change is rotation of the carboethoxy groups so that they are no longer in conjugation.

Finally, we would like to point out the utility of the external pressure parameter to unravel the complex pathways of electronically excited states. Pressure permits, among other things, the variation in continuous way of the relative energies between states. Since the rates of many phenomena depend in one way or another on the energy gap, pressure permits the systematic probing of selective decay modes.

**Acknowledgment.** This research was supported in part by the Energy Research and Development Administration under Contract EY-76-C-02-1198, in part by a grant from the Research Corporation, and in part by the donors of the Petroleum Research Fund, administered by the American Chemical Society.

## References and Notes

- (1) J. B. Birks, *Chem. Phys. Lett.*, **17**, 370 (1972).
- (2) D. Huppert, J. Jortner, and P. M. Rentzepis, *J. Chem. Phys.*, **56**, 4826 (1972).
- (3) P. M. Rentzepis, *Chem. Phys. Lett.*, **3**, 717 (1969); P. Wirth, S. Schneider, and F. Dorr, *ibid.*, **42**, 482 (1976); J. P. Heritage and A. Penzkofer, *ibid.*, **44**, 76 (1976).
- (4) E. Drent, G. M. Van Der Deijl, and P. J. Zandstra, *Chem. Phys. Lett.*, **2**, 526 (1968).
- (5) For example see D. J. Mitchell, G. B. Schuster, and H. G. Drickamer, *J. Am. Chem. Soc.*, **99**, 1145 (1977).

- (6) B. Y. Okamoto and H. G. Drickamer, *J. Chem. Phys.*, **61**, 2870 (1974).
- (7) T. Nozoe, S. Seto, S. Matsumura, and Y. Murase, *Bull. Chem. Soc. Jpn.*, **35**, 1179 (1962); T. Nozoe, S. Seto, and S. Matsumura, *ibid.*, **35**, 1990 (1962).
- (8) G. Eber, F. Gruneis, S. Schneider, and F. Dorr, *Chem. Phys. Lett.*, **29**, 397 (1974).
- (9) W. D. Drotning and H. G. Drickamer, *Phys. Rev. B*, **13**, 4568 (1976).
- (10) C. E. Tyner, personal communication.
- (11) W. H. Melluish, *J. Opt. Soc. Am.*, **54**, 183 (1964).
- (12) B. A. Baldwin and H. W. Offen, *J. Chem. Phys.*, **49**, 2933 (1968).
- (13) C. W. Struck and W. H. Fonger, *J. Lumin.*, **10**, 1 (1975).
- (14) H. W. Offen in "Organic Molecular Photophysics", Vol. 1, J. B. Birks, Ed., Wiley, New York, N.Y., 1973.
- (15) R. Englman and J. Jortner, *Mol. Phys.*, **18**, 145 (1970).
- (16) W. Siebrand and D. F. Williams, *J. Chem. Phys.*, **49**, 1860 (1968).
- (17) S. Murata, C. Iwanga, T. Toda, and H. Kokubun, *Chem. Phys. Lett.*, **13**, 101 (1972).
- (18) P. W. Bridgman, *Proc. Am. Acad. Arts. Sci.*, **61**, 57 (1926).
- (19) H. Yamaguchi, T. Ikeda, and H. Mametska, *Bull. Chem. Soc. Jpn.*, **49**, 1762 (1976).
- (20) W. W. Robertson and A. D. King, Jr., *J. Chem. Phys.*, **34**, 1511 (1961).
- (21) H. N. Offen and D. E. Hein, *J. Chem. Phys.*, **50**, 5274 (1969).

# Conformational Characteristics of Rigid Cyclic Nucleotides. 2. The Solution Conformation of $\alpha$ -Nucleoside 3',5'-Cyclic Monophosphates and the Role of the 2'-Hydroxyl Group<sup>1</sup>

Malcolm MacCoss,\*<sup>2a</sup> Fouad S. Ezra,<sup>2a</sup> Morris J. Robins,<sup>2b</sup> and Steven S. Danyluk<sup>2a</sup>

*Contribution from the Division of Biological and Medical Research, Argonne National Laboratory, Argonne, Illinois 60439, and Department of Chemistry, The University of Alberta, Edmonton, Alberta, Canada T6G 2G2. Received April 28, 1977*

**Abstract:** The first detailed study has been made of the 220-MHz NMR spectra of  $\alpha$ -adenosine 3',5'-cyclic monophosphate (I,  $\alpha$ -cAMP),  $\alpha$ -uridine 3',5'-cyclic monophosphate (II,  $\alpha$ -cUMP),  $\alpha$ -cytidine 3',5'-cyclic monophosphate (III,  $\alpha$ -cCMP),  $\alpha$ -deoxyadenosine 3',5'-cyclic monophosphate (IV,  $\alpha$ -cdAMP),  $\alpha$ -5,6-dihydrouridine 3',5'-cyclic monophosphate (V,  $\alpha$ -cDHUMP), and  $\beta$ -5,6-dihydrouridine 3',5'-cyclic monophosphate (VI,  $\beta$ -cDHUMP) in D<sub>2</sub>O solution. Analyses of the spectra of I-III were aided by the use of europium chloride as a shift reagent. A conformational analysis showed the sugar moieties of I-III to exhibit a conformation in the range  ${}^2T^3$  to  ${}^3T_2$  with an unusually high distortion from planarity, in contrast to the  $\beta$  anomers which prefer  ${}^3E$  to  ${}^4T^3$  and the acyclic mononucleotides which show a  ${}^2E \rightleftharpoons {}^3E$  equilibrium. This change in the preferred conformation is attributed to a repulsive interaction between the 2'-hydroxyl and the base. Removal of the 2'-hydroxyl group eliminates this interaction and causes a relaxation to a less strained system. This is clearly demonstrated in the sugar ring conformation of IV which exhibits a  ${}^3E$  to  ${}^4E$  pucker and a puckering amplitude that is less than in the ribo series. Hydrogenation of the pyrimidine ring of II and  $\beta$ -cUMP gave the 5,6-dihydro products V and VI. VI exhibits preference for a  ${}^3E$  to  ${}^4T^3$  ribose ring conformation and in the case of V the 2'-hydroxyl-base interaction is markedly reduced owing to the increased flexibility of the aglycon. This results in a relaxation of the sugar ring conformation from the  ${}^2T^3$  to  ${}^3T_2$  in I-III back toward the  ${}^3E$  to  ${}^4T^3$  conformation found in the  $\beta$  anomers. Saturation of the base is not as effective as removal of the 2'-hydroxyl group in relieving the strain in these rigid systems. The phosphate ring is found to be in a flattened chair form in all cases. A detailed discussion is presented for chemical shift differences for particular protons in anomeric pairs.

In recent years, the conformational properties of nucleoside and nucleotide derivatives have been extensively studied by x-ray<sup>3</sup> and NMR methods.<sup>4</sup> The conformational properties of the flexible molecules such as nucleoside monophosphates and nucleoside 2',3'-cyclic monophosphates have been shown to be best represented in solution as a dynamic equilibrium between various conformers.<sup>4</sup> For example, the sugar conformation in such derivatives is usually expressed as a  ${}^2E \rightleftharpoons {}^3E$  equilibrium, and structural modifications to the molecule have been shown to affect the position of this equilibrium.<sup>5,6</sup>

An approach with considerable merit for defining specific conformational features utilizes derivatives in which this equilibrium is eliminated by the formation of a rigid ring system. This allows a simpler evaluation of particular intramolecular interactions<sup>7</sup> and of the shielding properties of hydroxyl groups on the sugar ring protons. The  $\beta$ -nucleoside 3',5'-cyclic

monophosphates are of biological importance,<sup>8</sup> and structurally they contain a six-membered phosphate ring fused trans (1,2) to a five-membered sugar ring. This produces a rigid bicyclic system with the sugar held in a  ${}^3E$  to  ${}^4T^3$  conformation.<sup>7,9</sup> Other rigid cyclic nucleotides which have been rigorously examined by NMR methods include 9-( $\beta$ -D-xylofuranosyl)adenine 3',5'-cyclic monophosphates<sup>10</sup> [possessing a six-membered phosphate ring fused cis (1,2) to a five-membered sugar ring] and the 2',5'-cyclic monophosphates of 1-( $\beta$ -D-arabinofuranosyl)cytosine<sup>9b,11</sup> and 9-( $\beta$ -D-arabinofuranosyl)adenine<sup>10</sup> [possessing a seven-membered phosphate ring fused cis (1,3) to a five-membered sugar ring]. Another series of derivatives which are structurally rigid is the anhydronucleosides, and these too have been well studied by NMR methods.<sup>7,12</sup>

A question of some significance is the influence of the 2'-